A sub-canopy structure for simulating oil palm in the Community Land Model (CLM-Palm): phenology, allocation and yield

Yuanchao Fan[1,2,*], Olivier Roupsard[3,4], Martial Bernoux[5], Guerric Le Maire[3], Oleg Panferov[6], Martyna M. Kotowska[7], Alexander Knohl[1]

[1] University of Göttingen, Department of Bioclimatology, Büsgenweg 2, 37077 Göttingen, Germany

[2] AgroParisTech, SIBAGHE (Systèmes intégrés en Biologie, Agronomie, Géosciences, Hydrosciences et Environnement), 34093 Montpellier, France

[3] CIRAD, UMR Eco&Sols (Ecologie Fonctionnelle & Biogéochimie des Sols et des Agro-écosystèmes), 34060 Montpellier, France

[4] CATIE (Tropical Agricultural Centre for Research and Higher Education), 7170 Turrialba, Costa Rica

[5] IRD, UMR Eco&Sols, 34060 Montpellier, France

[6] University of Applied Sciences Bingen, 55411 Bingen am Rhein, Germany

[7] University of Göttingen, Department of Plant Ecology and Ecosystems Research, Untere Karspüle 2, 37073 Göttingen, Germany

*Correspondence author. E-mail: yfan1@uni-goettingen.de

Abstract: Towards an effort to quantify the effects of forests to oil palm conversion occurring in the tropics on land-atmosphere carbon, water and energy fluxes, we introduce a new perennial crop phenology and allocation sub-model (CLM-Palm) for simulating a palm plant functional type (PFT) within the framework of the Community Land Model. The CLM-Palm is tested here on oil palm only but is meant of generic interest for other palm crops (e.g. coconut). The oil palm has monopodial morphology and sequential phenology of around 40 stacked phytomers, each carrying a large leaf and a fruit bunch, forming a natural multilayer canopy. A sub-canopy phenological and physiological parameterization is thus developed, so that each phytomer has its own prognostic leaf growth and fruit yield capacity but with shared stem and root components. Phenology and carbon and nitrogen allocation operate on the different phytomers in parallel but at unsynchronized steps, separated by a thermal period. An important phenological phase is identified for the oil palm - the storage growth period of bud and "spear" leaves which are photosynthetically inactive before expansion. Agricultural practices such as transplanting, fertilization, and leaf pruning are represented. Parameters introduced for the oil palm were calibrated and validated with field measurements of leaf area index (LAI) and yield from Sumatra, Indonesia. In calibration with a mature oil palm plantation, the cumulative yields from 2005 to 2014 matched notably well between simulation and observation (mean percentage error = 3%). Simulated inter-annual dynamics of PFT-level and phytomer-level LAI were both within the range of field measurements. Validation from eight independent oil palm sites shows the ability of the model to adequately predict the average leaf growth and fruit yield across sites but also indicates that seasonal dynamics and small-scale site-to-site variability of yield are driven by processes not yet implemented in the model or reflected in the input data. The new sub-canopy structure and phenology and allocation functions in CLM-Palm allow exploring the effects of tropical land use change, from natural ecosystems to oil palm plantations, on carbon, water and energy cycles and regional climate.

1. Introduction

Land-use changes in South-East Asia's tropical regions have been accelerated by economy-driven expansion of oil palm (*Elaeis guineensis*) plantations since the 1990s (Miettinen et al., 2011). Oil palm is currently one of the most rapidly expanding crops in the world (Carrasco et al., 2014) and Indonesia as the largest global palm-oil producer is planning to double its oil-palm area from 9.7 million ha in 2009 to 18 million ha by 2020 (Koh and Ghazoul, 2010). Since oil palms favor a tropical-humid climate with consistently high temperatures and humidity, the plantation expansion has converted large areas of rainforest in Indonesia in the past two decades including those on carbon-rich peat soils (Carlson et al., 2012; Gunarso et al. 2013).

Undisturbed forests have long-lasting capacity to store carbon in comparison to disturbed or managed vegetation (Luyssaert et al., 2008). Tropical deforestation caused by the expansion of oil palm plantations has significant implications on above- and belowground carbon stocks (Kotowska et al., 2015a). However, the exact quantification of the forest – oil palm replacement effects is difficult as the greenhouse gas balance of oil palms is still uncertain due to incomplete monitoring of the dynamics of oil palm plantations (including young development stage), and lack of understanding of the carbon, nitrogen, water and energy exchange between oil palms, soil and the atmosphere at ecosystem scale. Besides that, the assessment of these processes in agricultural ecosystems is complicated by human activities e.g. crop management, including planting and pruning, irrigation and fertilization, litter and residues management, and yield outputs. One of the suitable tools for evaluating the feedback of oil palm expansion is ecosystem modelling. Although a series of agricultural models exist for simulating the growth and yield of oil palm such as OPSIM (van Kraalingen et al., 1989), ECOPALM (Combres et al., 2013), APSIM-Oil Palm (Huth et al., 2014), PALMSIM (Hoffmann et al., 2014), these models did not aim yet at the full picture of carbon, water and energy exchanges between land and atmosphere and remain to be coupled with climate

models. Given the current and potential large-scale deforestation driven by the expansion of oil palm plantations, the ecosystem services such as yield, carbon sequestration, microclimate, energy and water balance of this new managed oil palm landscape have to be evaluated in order to estimate the overall impact of land-use change on environment including regional and global climate.

Land surface modelling has been widely used to characterize the two-way interactions between climate and human activities in terrestrial ecosystems such as deforestation, agricultural expansion, and urbanization (Jin and Miller, 2011; Oleson et al., 2004). A variety of land models have been adapted to simulate land-atmosphere energy and matter exchanges for major crops such as the CLM, LPJmL, JULES, ORCHIDEE models, etc. The Community Land Model (CLM4.5) is the land component of the Community Earth System Model (CESM) (Oleson et al., 2013). The model represents the crop and naturally vegetated land units as patches of plant functional types (PFTs) defined by their key ecological functions (Bonan et al., 2002). However, most of the crops being simulated are annual crops such as wheat, corn, soybean, rice, etc. Their phenological cycles are usually represented as three stages of development from planting to leaf emergence, to fruit-fill and to harvest, all within a year. Attempts were also made to evaluate the climate effects of perennial crops, e.g. by extending the growing season of annuals (Georgescu et al., 2011). However the perennial crops such as oil palm, cacao, coffee, rubber, coconut, and other fruiting trees and their long-term biophysical processes are not represented in the above land models yet, despite the worldwide growing demand (FAO, 2013).

Oil palm is a perennial evergreen crop which can by described by the Corner's architectural model (Hallé et al., 1978). A number of phytomers, each carrying a large leaf and axillating a fruit bunch, emerge successively (nearly two per month) from a single meristem (the bud) at the top of a solitary stem. They form a multilayer canopy with old leaves progressively being covered by new ones, until being pruned at senescence. Each phytomer has its own

phenological stage and yield, according to respective position in the crown. The oil palm is productive for more than 25 years, including a juvenile stage of around 2 years. In order to capture the inter- and intra-annual dynamics of growth and yield and land-atmosphere energy, water and carbon fluxes in the oil palm system, a new structure and dimension detailing the phytomer-level phenology, carbon (C) and nitrogen (N) allocation and agricultural managements have to be added to the current integrated plant-level physiological parameterizations in the land models. This specific refinement needs to remain compliant with the current model structure though, and be simple to parameterize.

In this context, we develop a new CLM-Palm sub-model for simulating the growth, yield, and energy and material cycling of oil palm within the framework of CLM4.5. It introduces a sub-canopy phenological and physiological parameterization, so that multiple leaf and fruit components operate in parallel but at delayed steps. A phytomer in the model is meant to represent the average condition of an age-cohort of actual oil palm phytomers across the whole plantation landscape. The overall gross primary production (GPP) by leaves and carbon output by fruit harvests rely on the development trends of individual phytomers. The functions implemented for oil palm combine the characteristics of both trees and crops, such as the woody-like stem growth and turnover but the crop-like vegetative and reproductive allocations which enable fruit C and N output. Agricultural practices such as transplanting, fertilization, and leaf pruning are also represented.

The main objectives of this paper are to: i) describe the development of CLM-Palm including its phenology, carbon and nitrogen allocation, and yield output; ii) optimize model parameters using field-measured leaf area index (LAI) and observed long-term monthly yield data from a mature oil palm plantation in Sumatra, Indonesia; and iii) validate the model against independent data from eight oil palm plantations of different age in Sumatra, Indonesia.

2. Model development

For adequate description of oil palm functioning, we adapted the CLM crop phenology, allocation and vegetative structure subroutines to the monopodial morphology and sequential phenology of oil palm so that each phytomer evolves independently in growth and yield (Fig. 1). Their phenology sequence is determined by the phyllochron (the period in thermal time between initiations of two subsequent phytomers) (Table A1). A maximum of 40 phytomers and expanded leaves, each growing up to 7-m long, are usually maintained in plantations by pruning management. There are also around 60 initiated phytomers developing slowly inside the bud. The largest ones, already emerged at the top of the crown but unexpanded yet, are named "spear" leaves (Fig. 1a). Each phytomer can be considered a sub-PFT component that has its own prognostic leaf growth and fruit yield capacity but having 1) the stem and root components that are shared by all phytomers, 2) the soil water content, nitrogen resources, and resulting photosynthetic assimilates that are also shared and partitioned among all phytomers, and 3) a vertical structure of the foliage, with the youngest at the top and the oldest at the bottom of the canopy. Within a phytomer the fruit and leaf components do not compete for growth allocation because leaf growth usually finishes well before fruit-fill starts. However one phytomer could impact the other ones through competition for assimilates, which is controlled by the C and N allocation subroutine according to their respective phenological stages.

Here we describe only the new phenology, allocation and agricultural management functions developed for the oil palm. Photosynthesis, respiration, water and nitrogen cycles and other biophysical processes already implemented in CLM4.5 (Oleson et al., 2013) are not modified (except N retranslocation scheme) for the current study. The following diagram shows the new functions and their coupling with existing modules within the CLM4.5 framework (Fig. 2).

2.1. Phenology

Establishment of the oil palm plantation is implemented with two options: seed sowing and transplanting of seedlings. In this study, only the transplanting option is used. We design 7 phenological steps for the development of each phytomer: 1) leaf initiation; 2) start of leaf expansion; 3) leaf maturity; 4) start of fruit-fill; 5) fruit maturity and harvest; 6) start of leaf senescence; and 7) end of leaf senescence and pruning (Fig. 1b). The first two steps differentiate pre-expansion (heterotrophic) and post-expansion (autotrophic) leaf growth phases. The other steps control leaf and fruit developments independently so that leaf growth and maturity could be finished well before fruit-fill and leaf senescence could happen after fruit harvest according to field observations. The modified phenology subroutine controls the life cycle of each phytomer as well as the planting, stem and root turnover, vegetative maturity (start of fruiting) and final rotation (replanting) of the whole PFT. Details on the timing and implementation of oil palm phenology and nitrogen retranslocation during senescence are in the Supplementary materials. The main phenological parameters are in Table A1.

All phytomers are assumed to follow the same phenological steps, where the thermal length for each phase is measured by growing degree-days (GDD; White et al., 1997). For oil palm, a new GDD variable with 15 ℃ base temperature and 25 degree-days daily maximum (Corley and Tinker, 2003; Goh, 2000; Hormaza et al., 2012) is accumulated from planting (abbr. GDD_{15}). The phenological phases are signaled by respective GDD requirements, except that pruning is controlled by the maximum number of live phytomers according to plantation management (Table A1). Other processes in the model such as carbon and nitrogen allocation for growth of new tissues respond to this phenology scheme at both PFT level and phytomer level (section 2.2).

2.2. Carbon and Nitrogen allocation

171 In CLM, the fate of newly assimilated carbon from photosynthesis is determined by a coupled
172 C and N allocation routine. Potential allocation for new growth of various plant tissues is
173 calculated based on allocation coefficients and their allometric relationship (Table A2).

174 A two-step allocation scheme is designed for the sub-canopy phytomer structure and
175 according to the new phenology. First, available C (after subtracting respiration costs) is
176 partitioned to the root, stem, overall leaf, and overall fruit pools at the PFT level with respect
177 to their relative demands controlled by phenology. The C:N ratios for different tissues link C
178 demand and N demand so that a N down-regulation mechanism is enabled to rescale GPP and
179 C allocation if N availability from soil mineral N pool and retranslocated N pool does not
180 meet the demand. Then, the actual C and N allocated to the overall leaf or fruit is partitioned
181 between different phytomers at the sub-PFT level (Fig. 2). Details are described below.

182 2.2.1. PFT level allocation

183 C and N allocation at the PFT level is treated distinctly before and after oil palm reaches
184 vegetative maturity. At the juvenile stage before fruiting starts (i.e. $GDD_{15} < GDD_{min}$) all the
185 allocation goes to the vegetative components. The following equations are used to calculate
186 the allometric ratios for partitioning available C and N to the leaf, stem, and root pools.

187 $$A_{root} = a^i_{root} - (a^i_{root} - a^f_{root}) \frac{DPP}{Age_{max}}, \quad \text{(Eq. 1)}$$

188 $$A_{leaf} = f^i_{leaf} \times (1 - A_{root}) \quad \text{(Eq. 2)}$$

189 $$A_{stem} = 1 - A_{root} - A_{leaf} \quad \text{(Eq. 3)}$$

190 where $\frac{DPP}{Age_{max}} \leq 1$, DPP is the days past planting, and Age_{max} is the maximum plantation age
191 (~25 years). a^i_{root} and a^f_{root} are the initial and final allocation coefficients for roots and f^i_{leaf}

is the initial leaf allocation coefficient before fruiting (Table A2). Root and stem allocation ratios are calculated with Eqs. 1 and 3 for all ages and phenological stages of oil palm.

After fruiting begins, the new non-linear function is used for leaf allocation:

$$A_{leaf} = a_{leaf}^{2} - (a_{leaf}^{2} - a_{leaf}^{f}) \left(\frac{DPP - DPP_2}{Age_{max} \times d_{mat} - DPP_2}\right)^{a_{alloc}^{leaf}} \quad \text{(Eq. 4)}$$

where a_{leaf}^{2} equals the last value of A_{leaf} calculated right before fruit-fill starts and DPP_2 is the days past planting right before fruit-fill starts. d_{mat} controls the age when the leaf allocation ratio approaches its final value a_{leaf}^{f}, while d_{alloc}^{leaf} determines the shape of change (convex when $d_{alloc}^{leaf} < 1$; concave when $d_{alloc}^{leaf} > 1$). A_{leaf} stabilizes at a_{leaf}^{f} when $DPP \geq Age_{max} d_{mat}$,. The equations reflect changed vegetative allocation strategy that shifts resources to leaf for maintaining LAI and increasing photosynthetic productivity when fruiting starts. The three vegetative allocation ratios A_{leaf}, A_{stem} and A_{root} always sum to 1.

At the reproductive phase a fruit allocation ratio A_{fruit} is introduced, relative to the total vegetative allocation unity. To represent the dynamics of reproductive allocation effort of oil palm, we adapt the stem allocation scheme for woody PFTs in CLM, in which increasing net primary production (NPP) results in increased allocation ratio for the stem wood (Oleson et al., 2013). A similar formula is used for reproductive allocation of oil palm so that it increases with increasing NPP:

$$A_{fruit} = \frac{2}{1 + e^{-b(NPP_{mon} - 100)}} - a \quad \text{(Eq. 5)}$$

where NPP_{mon} is the monthly sum of NPP from the previous month calculated with a run-time accumulator in the model. The number 100 (gC/m^2/mon) is the base monthly NPP when the palm starts to yield (Kotowska et al., 2015a). Parameters *a* and *b* adjust the base allocation rate and the slope of curve, respectively (Table A2). This function generates a dynamic curve

of A_{fruit} increasing from the beginning of fruiting to full vegetative maturity ($0 \leq A_{fruit} \leq 2$), which is used in the allocation allometry to partition assimilates between vegetative and reproductive pools (Fig. 3).

2.2.2. Sub-PFT (phytomer) level allocation

Total leaf and fruit allocations are partitioned to the different phytomers according to their phenological stages. Fruit allocation per phytomer is calculated with a sink size index:

$$S_p^{fruit} = \frac{GDD_{15} - H_p^{F.fill}}{H_p^{F.mat} - H_p^{F.fill}}, \quad \text{(Eq. 6)}$$

where p stands for the phytomer number, $H_p^{F.fill}$ and $H_p^{F.mat}$ are the phenological indices for the start of fruit-fill and fruit maturity (with $H_p^{F.fill} \leq GDD_{15} \leq H_p^{F.mat}$). S_p^{fruit} increases from zero at the beginning of fruit-fill to the maximum of 1 right before harvest for each phytomer. This is because the oil palm fruit accumulates assimilates at increasing rate during development until the peak when it becomes ripe and oil synthesis dominates the demand (Corley and Tinker, 2003). The sum of S_p^{fruit} for all phytomers gives the total reproductive sink size index. Each phytomer receives a portion of fruit allocation by $\frac{S_p^{fruit}}{\sum_{p=1}^{n} S_p^{fruit}} \times A_{fruit}$, where A_{fruit} is the overall fruit allocation by Eq. 5.

An important allocation strategy for leaf is the division of displayed versus storage pools for the pre-expansion and post-expansion leaf growth phases. These two types of leaf C and N pools are distinct in that only the displayed pools contribute to LAI growth, whereas the storage pools support the growth of unexpanded phytomers, i.e. bud & spear leaves, which remain photosynthetically inactive. Total C and N allocation to the overall leaf pool is divided to the displayed and storage pools by a fraction lf_{disp} (Table A2) according to the following equation:

$$A_{leaf}^{display} = lf_{disp} \times A_{leaf}$$
$$A_{leaf}^{storage} = (1 - lf_{disp}) \times A_{leaf} \quad \text{(Eq. 7)}$$

The plant level $A_{leaf}^{display}$ and $A_{leaf}^{storage}$ are then distributed evenly to expanded and unexpanded phytomers, respectively, at each time step. When a phytomer enters the leaf expansion phase, C and N from its leaf storage pools transfer gradually to the displayed pools during the expansion period. Therefore, a transfer flux is added to the real-time allocation flux and they together contribute to the post-expansion leaf growth.

LAI is calculated only for each expanded phytomer according to a constant specific leaf area (SLA) and prognostic amount of leaf C accumulated by phytomer *n*. In case it reaches the prescribed maximum ($PLAI_{max}$), partitioning of leaf C and N allocation to this phytomer becomes zero.

2.3. Other parameterizations

Nitrogen retranslocation is performed exclusively during leaf senescence and stem turnover. A part of N from senescent leaves and from the portion of live stem that turns dead is remobilized to a separate N pool that feeds plant growth or reproductive demand. Nitrogen of fine roots is all moved to the litter pool during root turnover. We do not consider N retranslocation from live leaves, stem and roots specifically during grain-fill that is designed for annual crops (Drewniak et al., 2013) because oil palm has continuous fruit-fill year around at different phytomers.

The fertilization scheme for oil palm is adapted to the plantation management generally carried out in our study area, which applies fertilizer biannually, starting only 6 years after planting, assuming each fertilization event lasts one day. Currently CLM uses an unrealistically high denitrification rate under conditions of nitrogen saturation, e.g. after fertilization, which results in a 50% loss of any excess soil mineral nitrogen per day (Oleson

et al., 2013). This caused the simple biannual regular fertilization nearly useless because peak N demand by oil palm is hard to predict given its continuous fruiting and vegetative growth and most fertilized N is thus lost in several days. The high denitrification factor has been recognized as an artifact (Drewniak et al., 2013; Tang et al., 2013). According to a study on a banana plantation in the tropics (Veldkamp and Keller, 1997), around 8.5% of fertilized N is lost as nitrogen oxide (N_2O and NO). Accounting additionally for a larger amount of denitrification loss to gaseous N_2, we modified the daily denitrification rate from 0.5 to 0.001, which gives a 30% annual loss of N due to denitrification that matches global observations (Galloway et al., 2004).

The irrigation option is turned off because oil palm plantations in the study area are usually not irrigated. Other input parameters for oil palm such as its optical, morphological, and physiological characteristics are estimated based on a literature review and field observations and summarized in Table A3. Most of them are generalized over the life of oil palm.

3. Model evaluation

3.1. Site data

Two oil palm plantations in the Jambi province of Sumatra, Indonesia provide data for calibration. One is a mature industrial plantation at PTPN-VI (01 °41.6' S, 103 °23.5' E, 2186 ha) planted in 2002, which provides long-term monthly harvest data (2005 to 2014). Another is a 2-year young plantation at a nearby smallholder site Pompa Air (01 °50.1' S, 103 °17.7' E, 5.7 ha). The leaf area and dry weight at multiple growth stages were measured by sampling leaflets of phytomers at different ranks (+1 to +20) on a palm and repeating for 3 different ages within the two plantations. The input parameter SLA (Table A2) was derived from leaf area and dry weight (excluding the heavy rachis). The phytomer-level LAI was estimated based on the number of leaflets (90-300) per leaf of a certain rank and the PFT-level LAI was estimated by the number of expanded leaves (35-45) per palm of a certain age. In both cases,

284 a planting density of 156 palms per hectare (8m × 8m per palm) was used according to
285 observation.

286 Additionally, LAI, yield and NPP measurements from eight independent mature oil palm sites
287 (50m × 50m each, > 10 years old) were used for model validation. Four of these sites (HO1,
288 HO2, HO3, HO4) are located in the Harapan region nearby PTPN-VI, and another four (BO2,
289 BO3, BO4, BO5) are located in Bukit Duabelas region (02 °04' S, 102 °47' E), both in Jambi,
290 Sumatra. Fresh bunch harvest data were collected at these sites for a whole year from July
291 2013 to July 2014. Harvest records from both PTPN-VI and the 8 validation sites were
292 converted to harvested carbon (g C/m^2) with mean wet/dry weight ratio of 58.65 % and C
293 content 60.13 % per dry weight according to C:N analysis (Kotowska et al., 2015a). The oil
294 palm monthly NPP and its partitioning between fruit, leaf, stem and root were estimated
295 based on measurements of fruit yield (monthly), pruned leaves (monthly), stem increment
296 (every 6 month) and fine root samples (once in a interval of 6-8 month) at the eight sites
297 (Kotowska et al., 2015b).

298 The mean annual rainfall (the Worldclim database: http://www.worldclim.org (Hijmans et al.,
299 2005); average of 50 years) of the two investigated landscapes in Jambi Province was ~2567
300 mm y^{-1} in the Harapan region (including PTPN-VI) and ~2902 mm y^{-1} in the Bukit Duabelas
301 region. In both areas, May to September represented a markedly drier season (30% less
302 precipitation) in comparison to the rainy season between October and April. Air temperature
303 is relatively constant throughout the year with an annual average of 26.7 ℃. In both
304 landscapes, the principal soil types are Acrisols: in the Harapan landscape loam Acrisols
305 dominate, whereas in Bukit Duabelas the majority is clay Acrisol. Soil texture such as
306 sand/silt/clay ratios and soil organic matter C content were measured at multiply soil layers
307 (down to 2.5m) (Allen et al., 2015). They were used to create two sets of surface input data
308 for the Harapan (H) and Bukit Duabelas (B) regions separately.

309 **3.2. Model setup**

The model modifications and parameterizations were implemented according to CLM standards. A new sub-PFT dimension called *phytomer* was added to all the new variables so that the model can output history tapes of their values for each phytomer and prepare restart files for model stop and restart with bit-for-bit continuity. Simulations were set up in point mode (a single 0.5×0.5 degree grid) at every 30-min time step. A spin-up procedure (Koven et al., 2013) was followed to get a steady-state estimate of soil C and N pools before 1850, with broadleaf evergreen tropical forest PFT only. Simulation continued on this equilibrium condition but was forced with dynamic CO_2 and climate data until 1990. After 1990, the forest was replaced with the oil palm at a specific year of plantation establishment. The oil palm functions were then turned on and simulations continued until 2014.

A simulation from 2002 to 2014 at the PTPN-VI site was used for model calibration. Additional eight simulations were run for the sites HO1, HO2, HO3, HO4, BO2, BO3, BO4, BO5 with two types of surface input files (for soil texture) and two types of climate forcing files (3-hourly ERA Interim data, Dee et al., 2011) for the H and B plots, respectively. The simulations started from different years (1996, 1997, 1999, 2000, 2001, 2002, 2003, 2004) when the palms were planted at the individual sites. Outputs from these simulations were used to validate the model in terms of LAI and yield.

3.3. Calibration of key parameters

Both the PFT level and phytomer level LAI development were calibrated with field observations in 2014 from a chronosequence approach (space for time substitution) using oil palm samples of three different age and multiple phytomers of different rank (section 3.1). Simulated yield outputs (around twice per month) were calibrated with monthly harvest records of PTPN-VI plantation from 2005 to 2014. Cumulative yields were compared because the timing of harvest in the plantations was largely uncertain and varied depending on weather and other conditions.

To simplify model calibration, we focused on parameters related to the new phenology and allocation processes. Phenological parameters listed in Table A1 were determined according to field observations and existing knowledge about oil palm growth phenology (Combres et al., 2013; Corley and Tinker, 2003) as well as plantation management in Sumatra, Indonesia. Allocation coefficients in Table A2 were more uncertain and they were the key parameters to optimize in order to match observed LAI and yield dynamics.

Parameters related to photosynthesis, stomatal conductance and respirations were set at similar levels as those of other crops, except that leaf traits such as $PLAI_{max}$ and *SLA* were determined by field measurements. Other parameters such as C:N ratios of the leaf, stem, root and fruit components were also left as similar levels as other crop PFTs.

3.4. Sensitivity analysis

Performing a full sensitivity analysis of all parameters used in simulating oil palm (more than 100 parameters, though a majority are shared with natural vegetation and other crops) would be a challenging work. As with calibration, we limited the sensitivity analysis to a set of parameters introduced for the specific PFT and model structure designed for oil palm. Among the phenological parameters, *mxlivenp* (maximum number of expanded phytomers) and *phyllochron* (Table A1) are closely related to pruning frequency but they should not vary widely for a given oil palm breed and plantation condition. Therefore, they were fixed at the average level for the study sites in Jambi, Sumatra. GDD_{init} was kept to zero because only the transplanting scenario was considered for seedling establishment. We tested two hypotheses of phytomer level leaf development based on the other phenological parameters: 1) considering the leaf storage growth period, that is, the bud & spear leaf phase is explicitly simulated with the GDD parameters in Table A1 and lf_{disp} = 0.3 in Table A2; 2) excluding the storage growth period by setting GDD_{exp} = 0 and lf_{disp} = 1 so that leaf expands immediately after initiation and leaf C and N allocation all goes to the photosynthetic active pools.

The sensitivity of allocation and photosynthesis parameters in Table A2 were tested by adding or subtracting 10% or 30% to the baseline values (calibrated) one-by-one and calculating their effect on final cumulative yield at the end of simulation (December 2014). In fact, all the allocation parameters are interconnected because they co-determine photosynthesis capacity and respiration costs as partitioning to the different vegetative and reproductive components varies. This simple approach provides a starting point to identify sensitive parameters, although a more sophisticated sensitivity analysis is needed in the future.

Parameter $PLAI_{max}$ is only meant for error controlling, although in our simulations phytomer-level LAI never reached $PLAI_{max}$ (see Fig. 5 in results) because environmental constraints and nitrogen down-regulation already limited phytomer leaf growth well within the range. The C:N ratios and some photosynthesis and respiration parameters were evaluated thoroughly in Bilionis et al. (2015). Since we do not consider specific N retranslocation during fruit-fill, some C:N parameters are not used for oil palm and the aspect of N content in different plant tissues is not prioritized for this sensitivity analysis.

3.5. Validation

In this study, we only validated the model structure and model behavior on simulating aboveground C partitioning and flux as represented by LAI, fruit yield and NPP. Independent LAI, yield and monthly NPP data collected in 2013−2014 from the eight mature oil palm sites (H and B plots) were compared with eight simulations using the above model settings and calibrated parameters.

4. Results

4.1. Calibration with LAI and yield

In model calibration with the PTPN-VI plantation, the PFT-level LAI dynamics simulated by the model incorporating the pre-expansion phase matches well with the LAI measurements

for three different ages (Fig. 4). Simulated LAI for the PFT increases with age in a sigmoid relationship. The dynamics of LAI is also impacted by pruning and harvest events because oil palms invest around half of their assimilates into fruit yield. Oil palms are routinely pruned by farmers to maintain the maximum number of expanded leaves around 40. Hence, when yield begins 2-3 years after planting, LAI recurrently shows an immediate drop after pruning and then quickly recovers. Simulations without the pre-expansion storage growth phase show an unrealistic fast increase of LAI before 3 years old, much higher than observed in the field. At older age after yield begins, LAI drops drastically and recovers afterwards. Although the final LAI could stabilize at a similar level, the initial jump and drop of LAI at young stage do not match field observations and cannot be solved by adjusting parameters other than GDD_{exp}. Hereafter, all simulations were run using the pre-expansion phase.

The phytomer level LAI development is comparable with leaf samples from the field (Fig. 5). The two leaf samples at rank 5 (LAI = 0.085) and rank 20 (LAI = 0.122) of a mature oil palm in PTPN-VI (the two black triangles for 2014) are within the range of simulated values. The other sample at rank 25 (LAI = 0.04, for 2004) on a young oil palm in Pompa Air is lower than the simulated value. Each horizontal color bar clearly marks the post-expansion leaf phenology cycle, including gradual increment of photosynthetic LAI during phytomer development and gradual declining during senescence. The pre-expansion phase is not included in the figure but model outputs show that roughly 60-70% of leaf C in a phytomer is accumulated before leaf expansion, which is co-determined by the allocation ratio lf_{disp} and the lengths of two growth phases set by GDD_{exp} and $GDD_{L.mat}$. This is comparable to observations on coconut palm that dry mass of the oldest unexpanded leaf accounts for 60% of that of a mature leaf (Navarro et al., 2008). Only when the palm becomes mature, phytomer LAI could come closer to the prescribed $PLAI_{max}$ (0.165). However, during the whole growth period from 2002 to 2014 none of the phytomers have reached $PLAI_{max}$, which is the prognostic result of the carbon balance simulated by the model.

The cumulative yield of baseline simulation has overall high consistency with harvest records (Fig. 6). The mean percentage error (MPE) is only 3%. The slope of simulated curve increases slightly after 2008 when the LAI continues to increase and NPP reaches a high level (Fig. 3). The harvest records also show the same pattern after 2008 when heavy fertilization began (456 kg N/ha/yr).

The per-month harvest records exhibit strong zig-zag pattern (Fig. 7). One reason is that oil palms are harvested every 15-20 days and summarizing harvest events by calendar month would result in uneven harvest times per month, e.g. two harvests fall in a previous month and only one in the next month. Yet it still shows that harvests at PTPN-VI plantation dominated from October to December whereas in the earlier months of each year harvest amounts were significantly lower. The simulated amount of yield per harvest event has less seasonal fluctuation, but it responds to the fluctuation of precipitation (Fig. 7). A slight positive linear correlation exists between simulated yield and the mean precipitation of a 60-day period (corresponds to the main fruit-filling and oil synthesis period) before each harvest event (Pearson's r = 0.15). Examining the longer term year-to-year variability, a clear increasing trend of yield with increasing plantation age is captured by the model, largely matching field records since the plantation began to yield in 2005.

4.2. Sensitivity analysis

The leaf nitrogen fraction in Rubisco (F_{LNR}) is shown to be the most sensitive parameter (Fig. 8), because it determines the maximum rate of carboxylation at 25 ℃ (V_{cmax25}) together with *SLA* (also sensitive), foliage nitrogen concentration (CN_{leaf}, Table A3) and other constants. Given the fact that F_{LNR} should not vary widely in nature for a specific plant, we constrained this parameter within narrow boundaries to get a V_{cmax25} around 100, which is similar to that shared by all other crop PFTs (100.7) and higher than forests (around 60) in CLM. We fixed *SLA* to 0.013 by field measurements. The value is only representative of the photosynthetic leaflets. The initial root allocation ratio (a_{root}^{i}) has considerable influence on yield because it

modifies the overall respiration cost along the gradual declining trend of fine root growth across 25 years (Eq. 1). The final ratio (a_{root}^{f}) has limited effects because its baseline value (0.1) is set very low and thus the percentage changes are insignificant. The leaf allocation coefficients (f_{leaf}^{i}, a_{leaf}^{f}) are very sensitive parameters because they determine the magnitudes of LAI and GPP and consequently yield. The coefficients d_{mat} and d_{alloc}^{leaf} control the nonlinear curve of leaf development (Eq. 4) and hence the dynamics of NPP and that partitioned to fruits. They were calibrated to match both the LAI and yield dynamics. Increased F_{stem}^{live} results in higher proportion of live stem throughout life, given the fixed stem turnover rate, and therefore it brings higher respiration cost and lower yield. Decreasing the fruit allocation coefficient *a* results in a higher base rate of A_{fruit} according to Eq. 5, whereas increasing coefficient *b* brings up the rate of change and final magnitude of A_{fruit} if NPP rises continuously. Their relative influence on yield is lower than the leaf allocation coefficients because of the restriction by NPP dynamics (Eq. 5). Parameters lf_{disp} and *transplant* have negligible effects. lf_{disp} has to work together with the phenological parameter GDD_{exp} to give a reasonable size of spear leaves before expansion according to field observation. Varying the size of seedlings at transplanting by 10% or 30% does not alter the final yield, likely because the resulting initial LAI is still within a limited range (0.1~0.2) given the baseline value 0.15.

4.3. Model validation with independent dataset

The LAI development curves for the eight oil palm sites follow similar patterns since field transplanting in different years (Fig. 9a). The average LAI of the eight sites from the model is comparable with field measurement in 2014 (MPE = 10%, Fig. 9b). Small-scale variability from site to site is not well captured, given that microclimate was only prescribed as two categories for H and P plots respectively and all the plots followed the same fertilization subroutine in the model. There are large uncertainties in field LAI estimates because we did

not measure LAI at the plot level directly but only sampled leaf area and dry weight of individual phytomers and scaled the values up.

The simulated annual yields match closely with the average yield of the eight sites measured in 2013-2014 (MPE = −4%) but the model-predicted variability across the sites is much lower than field records (Fig. 10). Modelled yield generally increases with plantation age, which can be explained by the increasing fruit allocation rate A_{fruit} with increasing LAI and NPP (Fig. 3). We do not have data to test an aging decline function of growth and yield and assume the oil palm plantations remain productive for 25 years (Age_{max}) before replanting.

The simulated monthly NPP with the calibrated parameters for PTPN-VI site also closely corresponds to the average level of field measured NPP from the 8 independent validation sites with mature oil palms (Fig. 3).

5. Discussion

Calibration and validation with multiple site data demonstrate the utility of CLM-Palm and the sub-canopy structure for simulating the growth and yield of the unique oil palm plantation system within a land surface modeling context.

The pre-expansion phenological phase is proved necessary for simulating both phytomer-level and PFT-level LAI development in a prognostic manner. The leaf C storage pool provides an efficient buffer to support phytomer development and maintain overall LAI during fruiting. It also avoids an abnormally fast increase of LAI in the juvenile stage when C and N allocation is dedicated to the vegetative components. Without the leaf storage pool, the plant's canopy develops unrealistically fast at young age and then enters an emergent drop once fruit-fill begins (Fig. 4). This is because the plant becomes unable to sustain leaf growth just from its current photosynthetic assimilates when a large portion is allocated to fruits. Furthermore, differentiating the two phases could avoid abrupt increase in photosynthesis if a phytomer with full dry mass shifts from photosynthetically inactive to active status at one step.

For the similar purpose, we implement the leaf senescence phenology phase which gradually decreases the photosynthetic capacity of a leaf at the bottom layer of canopy so as to avoid drastic reduction in photosynthesis if the bottom leaves were turned off immediately.

Resource allocation patterns for perennial crops are more difficult to simulate than annual crops. For annuals, the LAI is often assumed to decline during grain-fill (Levis et al., 2012). However, the oil palm has to sustain a rather stable leaf area while partitioning a significant amount of C to the fruits. The balance between reproductive and vegetative allocations is crucial. The dynamics of A_{fruit} as a function of monthly NPP is meant to capture the increasing yield capacity of oil palms during maturing at favorable conditions (often the case in oil pam plantations). The average value of A_{fruit} was around 1 (Fig. 3), resulting a near 1:1 ratio to partition available assimilates to the reproductive and vegetative pools which matched closely with field observations (Kotowska et al., 2015a; Kotowska et al., 2015b). Under severe stress conditions, this NPP-related function can decrease fruit allocation and shift resources to the vegetative components. Our experiments (not shown here) confirmed that the dynamic function is more robust than a simple time-dependent or vegetation-size-dependent allocation function. Figure 3 also shows that the average rate of growth and productivity (NPP) of mature oil palms is reasonably captured by the model across different site conditions.

The phenology and allocation processes in land surface models are usually aimed to represent the average growth trend of a PFT at large spatial scale (Bonan et al., 2002; Drewniak et al., 2013). We made a step forward by comparing point simulations with multiple specific site observations. The model predicts well the average LAI development and yield across the Jambi region as well as monthly NPP of mature plantations. Yet it exhibits a limitation of the land surface modeling approach, that is, the difficulty to capture the large site-to-site variations. The discrepancy was very likely due to insufficient representation of management (e.g. fertilization, harvest and pruning cycles), which has been shown to be crucial for determining oil palm growth and yield (Euler et al., 2015). Other factors such as insects,

fungal infection, and possibly different oil palm progenies could also result in difference in the average size and number of leaves and fruits per palm, and they are not represented in the model. Water availability (precipitation) and soil condition were only prescribed as two categories of inputs for H and B plots, respectively. Especially the amount and timing of fertilization vary largely from plantation to plantation and from year to year but the model uses uniform fertilization for all plots (which is usually the case when modeling with a PFT). A more complex dynamic fertilization scheme could be devised and evaluated thoroughly with additional field data, which we lack at the moment.

The model well simulates year-to-year variability in yield (Fig. 7), in which the increasing trend is closely related to the fruit allocation function (Fig. 3) and LAI development (Fig. 4). The seasonal variability in simulated yield corresponds to the precipitation data but it is difficult to interpret the difference with monthly harvest records due to the artificial zig-zag pattern. The harvest records from plantations do not necessarily correspond to the amount of mature fruits along a phenological time scale due to varying harvest arrangements, e.g. fruits are not necessarily harvested when they are ideal for harvest, but when it is convenient. Observations of mature fruits on a tree basis (e.g. Navarro et al., 2008 on coconut) would be more suitable to compare with modeled yield, but such data are not available at our sites. Some studies have also demonstrated important physiological mechanisms on oil palm yield including inflorescence gender determination and abortion rates that both respond to seasonal climatic dynamics although with a time lag (Combres et al., 2013; Legros et al., 2009). The lack of representation of such physiological traits might affect the seasonal dynamics of yield simulated by our model. However, these mechanisms are rarely considered in a land surface modelling context. Nevertheless, the results correspond generally to the purpose of our modelling which is focused on the long-term climatological effects of oil palm agriculture. The correct representation of multi-year trend of carbon balance which we did reach is more important than the correct prediction of each yield. For latter the more agriculturally-oriented models should be used.

Overall, the sub-canopy phytomer-based structure, the extended phenological phases for a perennial crop PFT and the two-step allocation scheme are distinct from existing functions in land surface models. The phytomer configuration of CLM-Palm is similar to the one already implemented in other oil palm growth and yield models such as the APSIM-Oil Palm model (Huth et al., 2014) or the ECOPALM yield prediction model (Combres et al., 2013). But the implementation of this sub-canopy structure is the first attempt among land surface models. CLM-Palm incorporates the ability of yield prediction, like an agricultural model, beside that it allows the modeling of biophysical and biogeochemical processes as a land model should do, e.g. what is the whole fate of carbon in plant, soil and atmosphere if land surface composition changes from a natural system to the managed oil palm system? In a following study, a fuller picture of the carbon, water and energy fluxes over the oil palm landscape are examined with the CLM-Palm sub-model presented here and evaluated with Eddy Covariance flux observation data. We develop this palm module in the CLM framework as it allows coupling with climate models so that the feedbacks of oil palm expansion to climate can be simulated in future steps.

6. Conclusions

The development of CLM-Palm including canopy structure, phenology, and carbon and nitrogen allocation functions was proposed for modeling an important agricultural system in Indonesia. This paper demonstrates the ability of the new palm module to simulate the inter-annual dynamics of vegetative growth and fruit yield from field planting to full maturity of the plantation. The sub-canopy-scale phenology and allocation strategy are necessary for this perennial evergreen crop which yields continuously on multiple phytomers. The pre-expansion leaf storage growth phase is proved essential for buffering and balancing overall vegetative and reproductive growth. Average LAI, yield and NPP were satisfactorily simulated for multiple sites, which fulfills the main mission of a land surface modeling approach, that is, to represent the average conditions and dynamics of large-scale processes. On the other hand, simulating small-scale site-to-site variation (50m × 50m sites) requires

detailed input data on site conditions (e.g. microclimate, soil, and micro-topography) and plantation managements that are often not available thus limiting the applicability of the model at small scale. The point simulations here provide a starting point for calibration and validation at large scales.

To be run in a regional or global grid, the age class structure of plantations needs to be taken into account. This can be achieved by setting multiple replicates of the PFT for oil palm, each planted at a point of time at a certain grid. As a result, a series of oil palm cohorts developing at different grids could be configured with a transient PFT distribution dataset, which allows for a quantitative analysis of the effects of land-use changes, specifically rainforest to oil palm conversion, on carbon, water and energy fluxes. This will contribute to the land surface modeling community for simulating this structurally unique, economically and ecologically sensitive, and fast expanding oil palm land cover.

Acknowledgements:

This study was funded by the European Commission Erasmus Mundus FONASO Doctorate fellowship. Field trips were partly supported by the Collaborative Research Centre 990 (Ecological and Socioeconomic Functions of Tropical Lowland Rainforest Transformation Systems (Sumatra, Indonesia)) funded by the German Research Foundation (DFG). We are grateful to Kara Allen (University of Göttingen, Germany), Dr. Bambang Irawan (University of Jambi, Indonesia) and the PTPN-VI plantation in Jambi for providing field data on oil palm. The source code of the post-4.5 version CLM model was provided by Dr. Samuel Levis from National Center for Atmospheric Research (NCAR), Boulder, CO, USA.

Figures

(a)

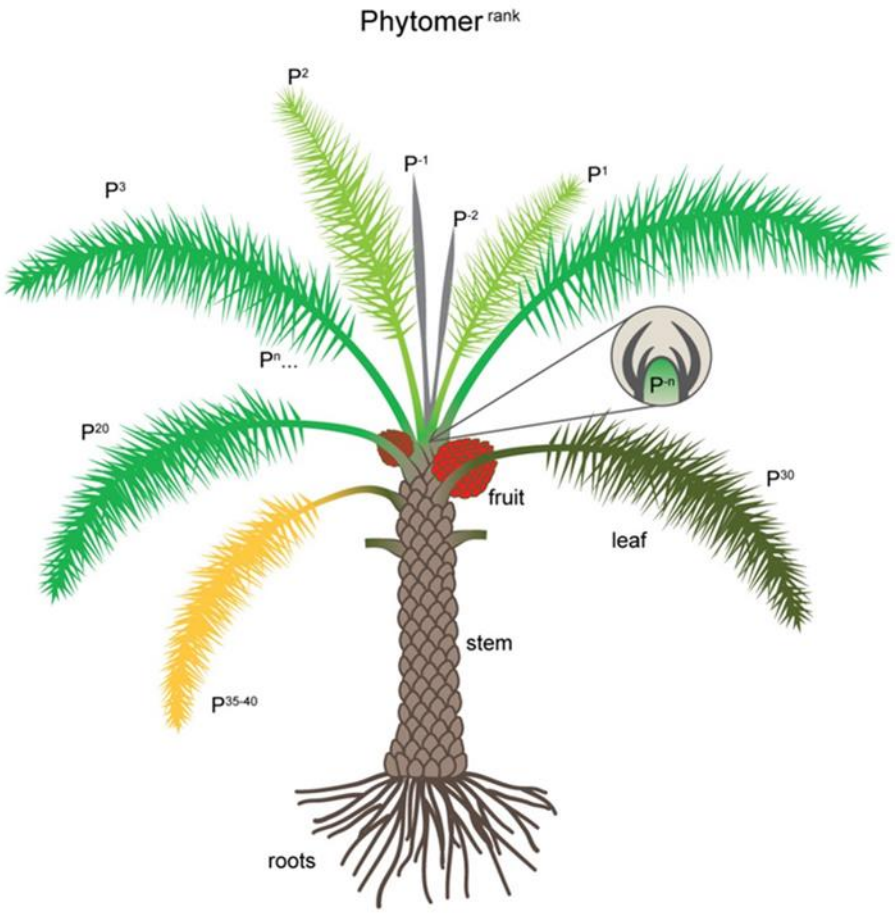
Phytomer rank
P2
P-1
P1
P3
P-2
Pn...
P-n
P20
P30
fruit
leaf
stem
P35-40
roots

(b)

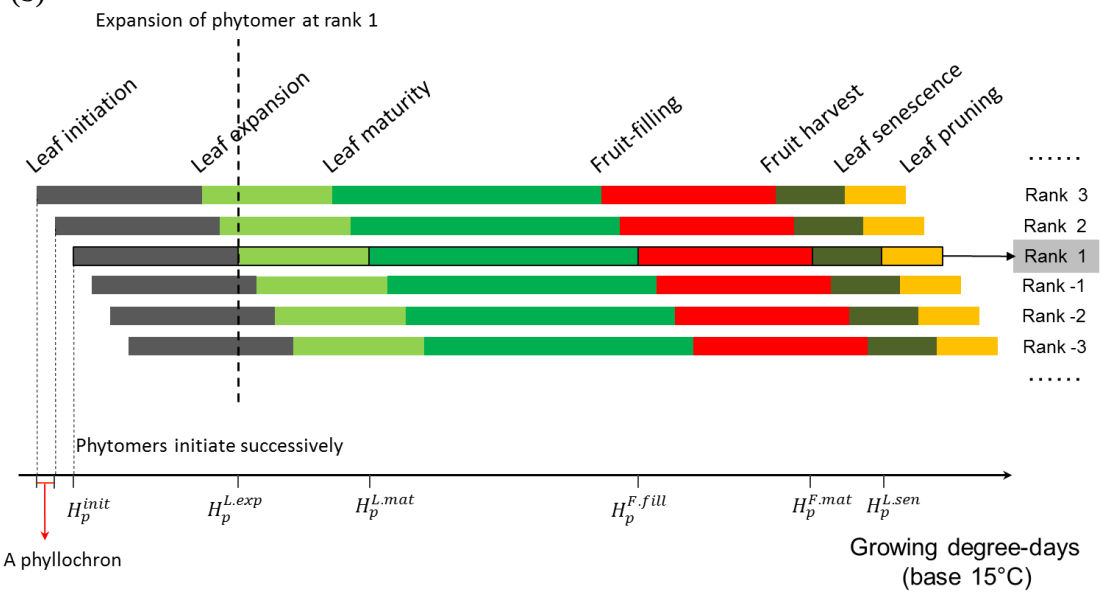
Expansion of phytomer at rank 1
Leaf initiation
Leaf expansion
Leaf maturity
Fruit-filling
Fruit harvest
Leaf senescence
Leaf pruning
Rank 3
Rank 2
Rank 1
Rank -1
Rank -2
Rank -3
Phytomers initiate successively
H_p^{init}
$H_p^{L.exp}$
$H_p^{L.mat}$
$H_p^{F.fill}$
$H_p^{F.mat}$
$H_p^{L.sen}$
A phyllochron
Growing degree-days
(base 15°C)

Fig. 1. (a) New sub-canopy phytomer structure for oil palm within CLM-Palm. P^1 to P^n indicate expanded phytomers and P^{-1} to P^{-n} at the top indicate unexpanded phytomers packed in the bud. Each phytomer has its own phenology, represented by different colors corresponding to: (b) the phytomer phenology: from initiation to leaf expansion, to leaf maturity, to fruit-fill, to harvest, to senescence and to pruning. Phytomers initiate successively according to the phyllochron (the period in heat unit between initiations of two subsequent phytomers). Detailed phenology description is in Supplementary materials.

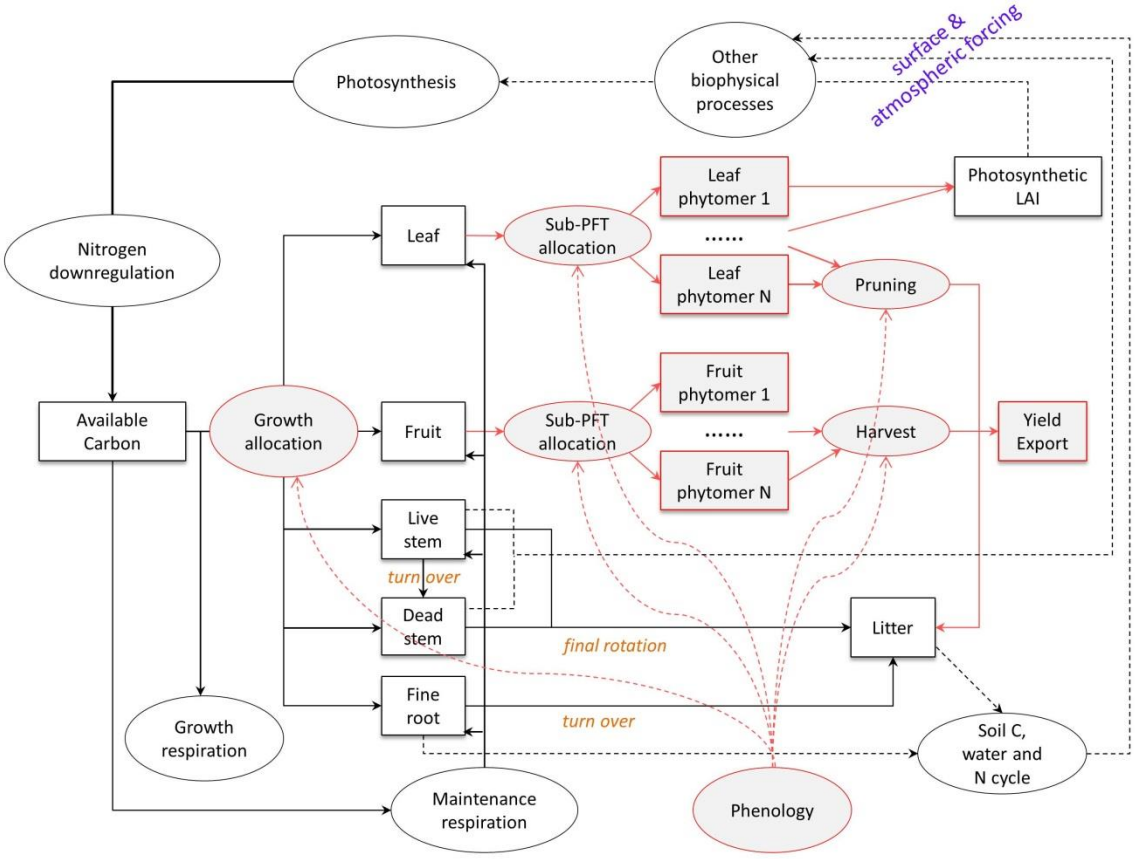

Fig. 2. Original and modified structure and functions for developing CLM-Palm in the framework of CLM4.5. Original functions from CLM4.5 are represented in black. New functions designed for CLM-Palm are represented in red, including phenology, allocation, pruning, fruit harvest and export, as well as the sub-canopy structure.

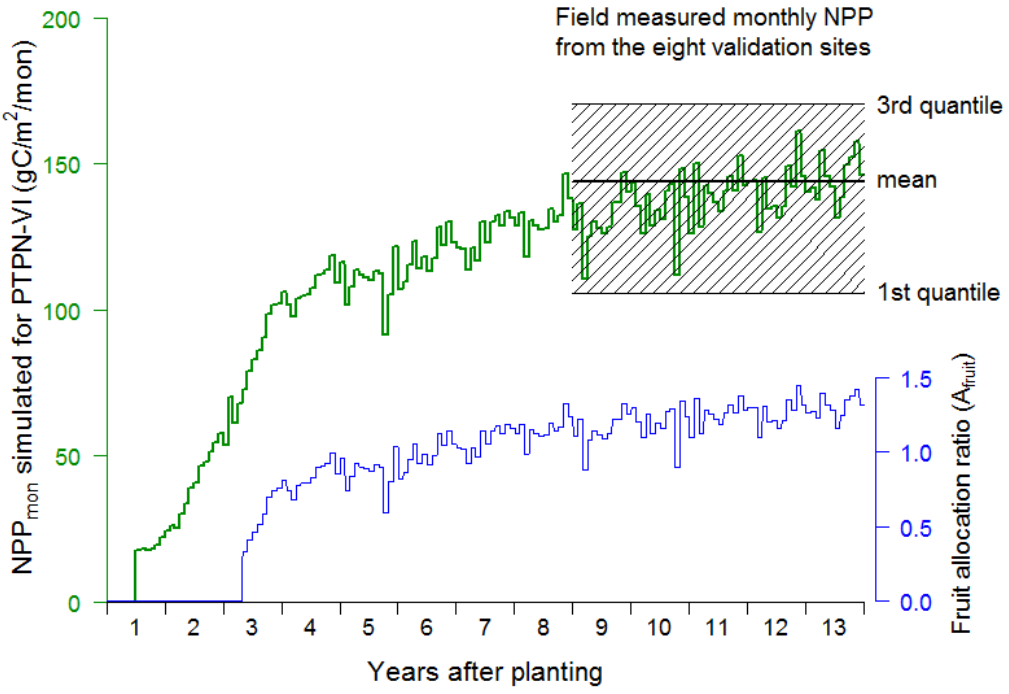

604

605 Fig. 3. Time course of reproductive allocation rate (blue line) in relation to monthly NPP from
606 the previous month (NPP_{mon}, green line) according to Eq. 5. A_{fruit} is relative to the vegetative
607 unity ($A_{leaf} + A_{stem} + A_{root} = 1$ and $0 \leq A_{fruit} \leq 2$). The NPP_{mon} was simulated with
608 calibrated parameters for the PTPN-VI site and was compared with field measured monthly
609 NPP from the 8 validation sites in Harapan and Bukit Duabelas regions.

610

611

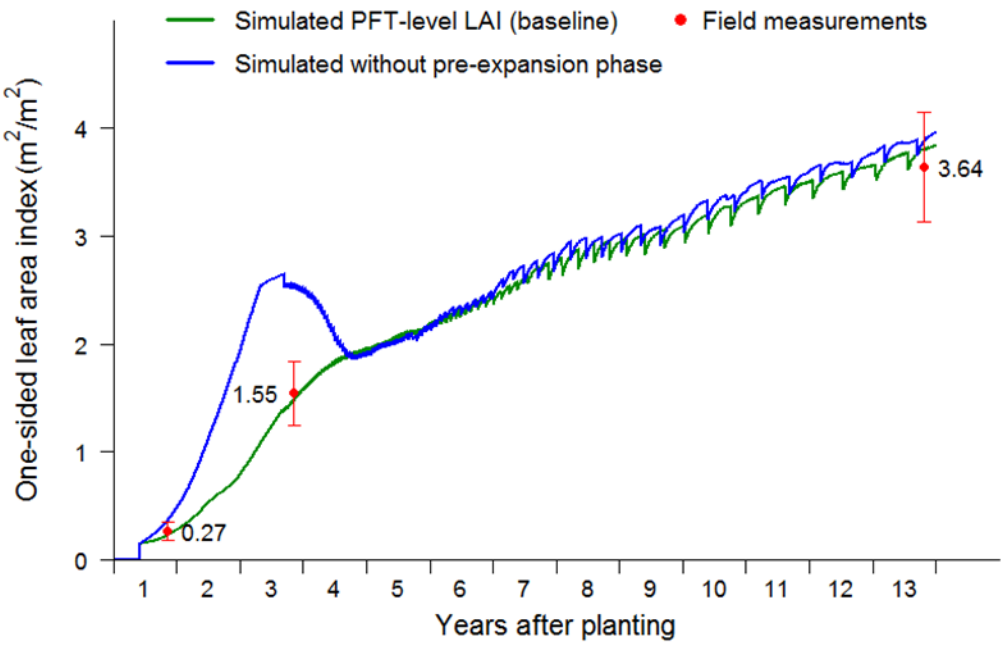

612

613 Fig. 4. PFT-level LAI simulated by CLM-Palm, with and without the pre-expansion growth
614 phase in the phytomer phenology and compared to field measurements used for calibration.
615 The initial sudden increase at year 1 represents transplanting from nursery. The sharp drops
616 mark pruning events.

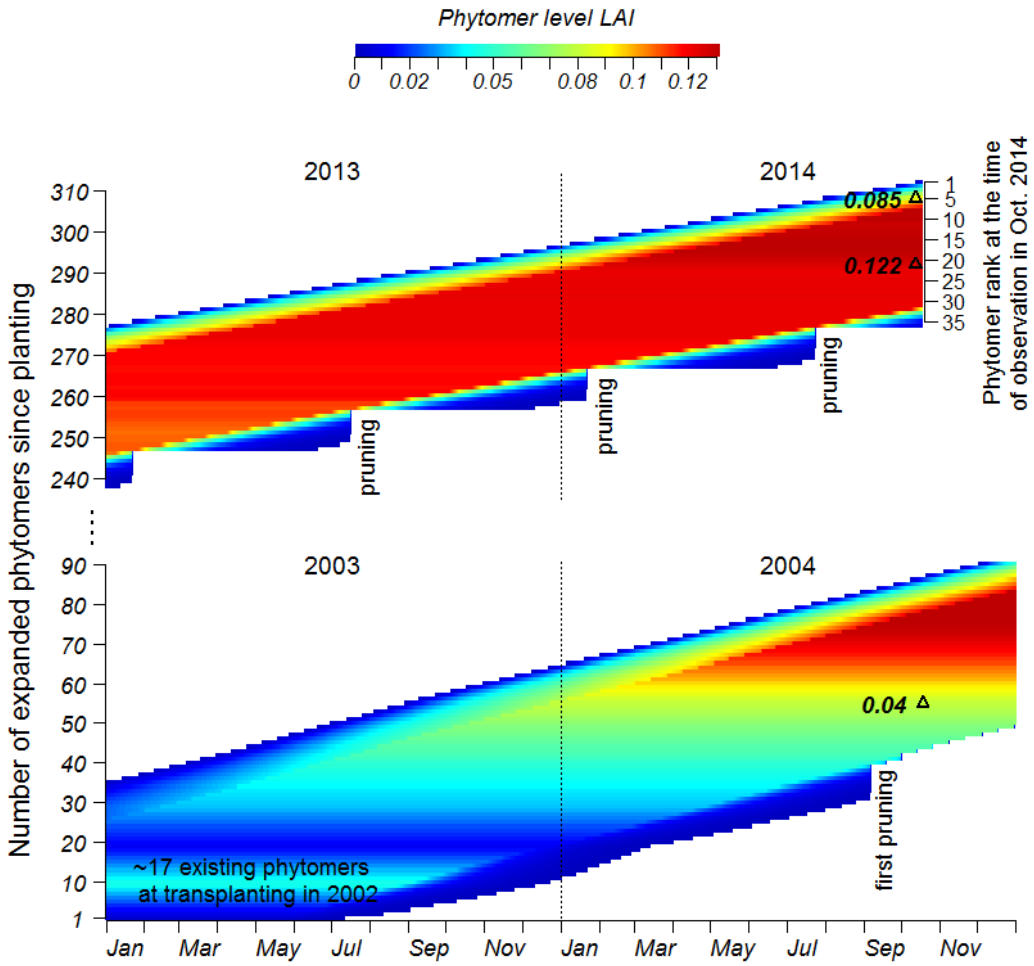

Fig. 5. Simulated phytomer level LAI dynamics (horizontal color bar) compared with field observations (black triangles with measured LAI value). The newly expanded phytomer at a given point of time has a rank of 1. Each horizontal bar represents the life cycle of a phytomer after leaf expansion. Phytomers emerge in sequence and the y-axis gives the total number of phytomers that have expanded since transplanting in the field. Senescent phytomers are pruned.

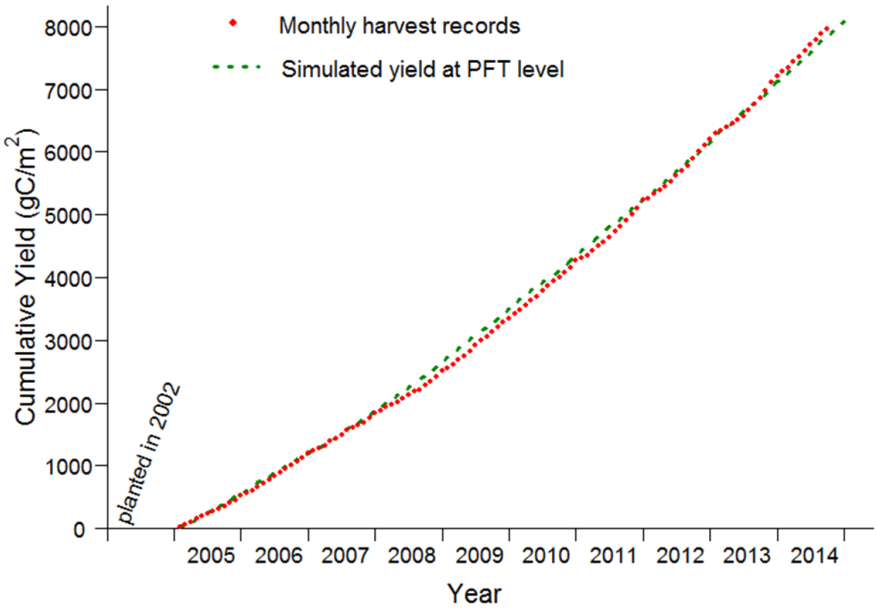

Fig. 6. Simulated PFT-level yield compared with monthly harvest data (2005-2014) from the calibration site PTPN-VI in Jambi, Sumatra. CLM-Palm represents multiple harvests (about twice per month) from different phytomers throughout time. The cumulative harvest amount from the model matches well with field records (MPE = 3%).

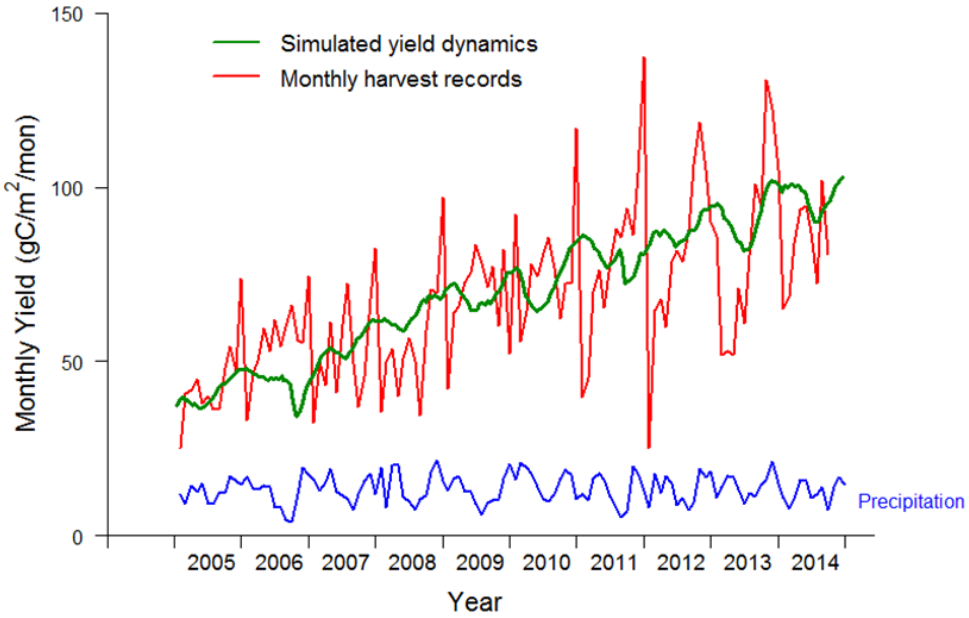

Fig. 7. Simulated and observed monthly yield at PTPN-VI compared with precipitation data. The modeled yield outputs are per harvest event (every 15-20 days depending on the phyllochron), while harvest records are the summary of harvest events per month. The model output is thus rescaled to show the monthly trend of yield that matches the mean of harvest records, given that the cumulative yields are almost the same between simulation and observation as shown in Fig. 6.

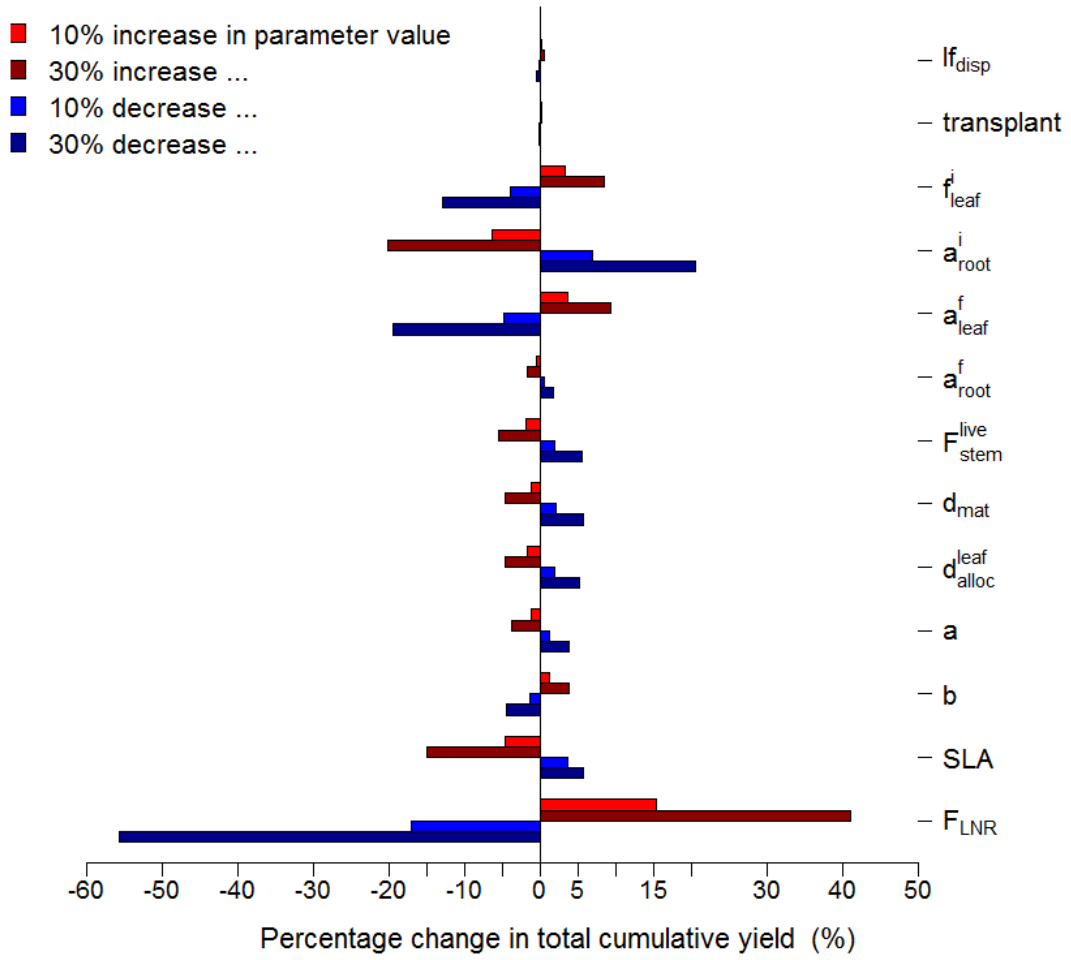

636

637 Fig. 8. Sensitivity analysis of key allocation parameters in regard of the cumulative yield at
638 the end of simulation, with two magnitudes of change in the value of a parameter one-by-one
639 while others are hold at the baseline values in Table A2.

640

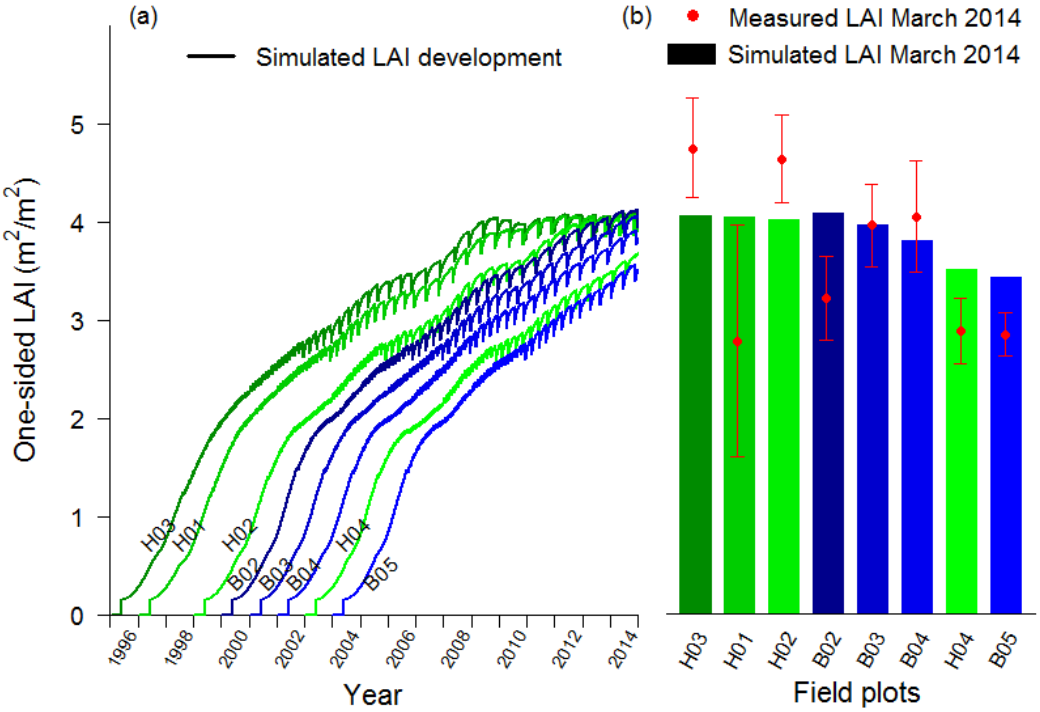

641

642 Fig. 9. Validation of LAI with 8 independent oil palm sites (sequence in plantation age) from
643 the Harapan (H) and Bukit Duabelas (B) regions: (a) shows the LAI development of each site
644 simulated by the model since planting; (b) shows the comparison of field measured LAI in
645 2014 with model.

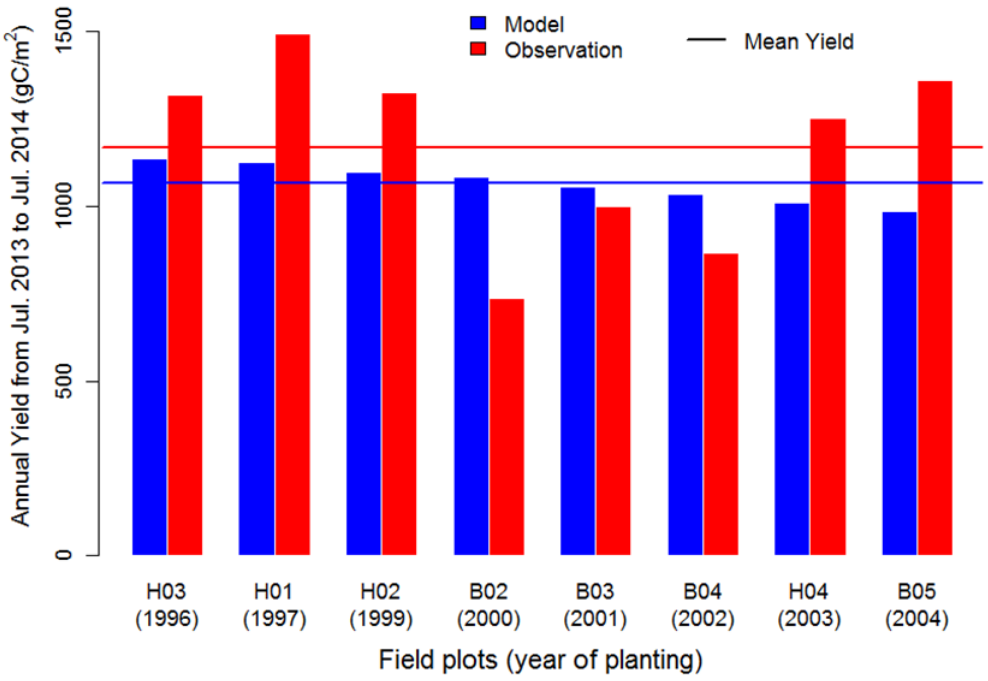

646

647 Fig. 10. Validation of yield with 8 independent oil palm sites from the Harapan (H) and Bukit
648 Duabelas (B) regions. The model predicted mean yield matches well with site average but
649 site-to-site variability due to management difference was not reflected by simulation.

Appendix A

Summary of main parameters

Table A1. Summary of new phenological parameters introduced for oil palm in the phenology subroutine. The default values were determined by calibration and with reference to field observations and literatures on oil palm (Combres et al., 2013; Corley and Tinker, 2003; Hormaza et al., 2012; Legros et al., 2009).

Parameter	Default	Min	Max	Explanation (Unit)
GDD_{init}	0	0	1500	GDD needed from planting to the first phytomer initiation (°days). Initiation refers to the start of active accumulation of leaf C. A value 0 implies transplanting.
GDD_{exp}	1550	0	8000	GDD needed from leaf initiation to start of leaf expansion for each phytomer (pre-expansion) (°days)
$GDD_{L.mat}$	1250	500	1600	GDD needed from start of leaf expansion to leaf maturity for each phytomer (post-expansion) (°days)
$GDD_{F.fill}$	3800	3500	4200	GDD needed from start of leaf expansion to beginning of fruit-fill for each phytomer (°days)
$GDD_{F.mat}$	5200	4500	6500	GDD needed from start of leaf expansion to fruit maturity and harvest for each phytomer (°days)
$GDD_{L.sen}$	6000	5000	8000	GDD needed from start of leaf expansion to beginning of senescence for each phytomer (°days)
GDD_{end}	6650	5600	9000	GDD needed from start of leaf expansion to end of senescence for each phytomer (°days)
GDD_{min}	7500	6000	10000	GDD needed from planting to the beginning of first fruit-fill (°days)
Age_{max}	25	20	30	Maximum plantation age (productive period) from planting to final rotation /replanting (years)
mxlivenp	40	30	50	Maximum number of expanded phytomers coexisting on a palm
phyllochron	130	100	160	Initial phyllochron (=plastochron): the period in heat unit between the initiations of two successive phytomers. The value increases to 1.5 times, i.e. 195, at 10-year old (°days)

Table A2. Summary of parameters involved in C and N allocation. The default values were determined by calibration and with reference to field measurements (Kotowska et al., 2015a).

Parameter	Defaults	Min	Max	Explanation (Unit)
$*lf_{disp}$	0.3	0.1	1	Fraction of C and N allocated to the displayed leaf pool
*transplant	0.15	0	0.3	Initial total LAI assigned to existing expanded phytomers at transplanting. Value 0 implies planting as seeds.
f_{leaf}^{i}	0.16	0	1	Initial value of leaf allocation coefficient before the first fruit-fill
a_{root}^{i}	0.3	0	1	Initial value of root allocation coefficient before the first fruit-fill
a_{leaf}^{f}	0.27	0	1	Final value of leaf allocation coefficient after vegetative maturity
a_{root}^{f}	0.1	0	1	Final value of root allocation coefficient after vegetative maturity
F_{stem}^{live}	0.15	0	1	Fraction of new stem allocation that goes to live stem tissues, the rest to metabolically inactive stem tissues
d_{mat}	0.5	0.1	1	Factor to control the age when the leaf allocation ratio stabilizes at a_{leaf}^{f} according to Eq. 4
d_{alloc}^{leaf}	0.6	0	5	Factor to control the nonlinear function in Eq. 4. Values < 1 give a convex curve and those > 1 give a concave curve. Value 1 gives a linear function.
*a	0.28	0	1	Parameter *a* for fruit allocation coefficient A_{fruit} in Eq. 5
*b	0.03	0	1	Parameter *b* for fruit allocation coefficient A_{fruit} in Eq. 5
$PLAI_{max}$	0.165	0.1	0.2	Maximum LAI of a single phytomer (m^2 m^{-2})
SLA	0.013	0.01	0.015	Specific leaf area (m^2 g^{-1} C)
F_{LNR}	0.0762	0.05	0.1	Fraction of leaf nitrogen in Rubisco enzyme. Used together with *SLA* to calculate V_{cmax25} (g N Rubisco g^{-1} N)

*New parameters introduced for oil palm. Others are existing parameters in CLM but mostly are redefined or used in changed context.

658 Table A3. Other optical, morphological, and physiological parameters for oil palm.

Parameter	Value	Definition (Unit)	Comments
CN_{leaf}	25	Leaf carbon-to-nitrogen ratio (g C g^{-1} N)	Same as all other PFTs
CN_{root}	42	Root carbon-to-nitrogen ratio (g C g^{-1} N)	Same as all other PFTs
CN_{livewd}	50	Live stem carbon-to-nitrogen ratio (g C g^{-1} N)	Same as all other PFTs
CN_{deadwd}	500	Dead stem carbon-to-nitrogen ratio (g C g^{-1} N)	Same as all other PFTs
CN_{lflit}	50	Leaf litter carbon-to-nitrogen ratio (g C g^{-1} N)	Same as all other PFTs
CN_{fruit}	75	Fruit carbon-to-nitrogen ratio (g C g^{-1} N)	Higher than the value 50 for other crops because of high oil content in palm fruit
$r_{vis/nir}^{leaf}$	0.09/0.45	Leaf reflectance in the visible (VIS) or near-infrared (NIR) bands	Values adjusted in-between trees and crops
$r_{vis/nir}^{stem}$	0.16/ 0.39	Stem reflectance in the visible or near-infrared bands	Values adjusted in-between trees and crops
$\tau_{vis/nir}^{leaf}$	0.05/0.25	Leaf transmittance in the visible or near-infrared bands	Values adjusted in-between trees and crops
$\tau_{vis/nir}^{stem}$	0.001/ 0.001	Stem transmittance in the visible or near-infrared bands	Values adjusted in-between trees and crops
χ_L	0.6	Leaf angle index to calculate optical depth of direct beam (from 0 = random leaves to 1 = horizontal leaves; –1 = vertical leaves)	Average leaf angle according to field observation
taper	50	Ratio of stem height to radius-at-breast-height	Field observation. Used together with *stocking* and *dwood* to calculate canopy top and bottom heights.
stocking	150	Number of palms per hectare (stems ha^{-2})	Field observation. Used to calculate stem area index (SAI) by: $SAI = 0.05 \times LAI \times stocking$.

dwood	100000	Wood density (gC m^{-3})	Similar as coconut palm (O. Roupsard, personal communication)
R_{z0m}	0.065	Ratio of momentum roughness length to canopy top height	T. June, personal communication
R_d	0.67	Ratio of displacement height to canopy top height	T. June, personal communication

References

Allen, K., Corre, M. D., Tjoa, A., and Veldkamp, E.: Soil nitrogen-cycling responses to conversion of lowland forests to oil palm and rubber plantations in Sumatra, Indonesia, PLoS ONE, 10(7), e0133325, doi:10.1371/journal.pone.0133325, 2015

Bilionis, I., Drewniak, B. A., and Constantinescu, E. M.: Crop physiology calibration in CLM, Geoscientific Model Development, 8(4), 1071-1083, 2015.

Bonan, G. B., Levis, S., Kergoat, L., and Oleson, K. W.: Landscapes as patches of plant functional types: An integrated concept for climate and ecosystem models, Global Biogeochemical Cycles, 16 (2), 1021-1051, 2002.

Carlson, K. M., Curran, L. M., Asner, G. P., Pittman, A. M., Trigg, S. N., and Adeney, J. M.: Carbon emissions from forest conversion by Kalimantan oil palm plantations, Nature Clim. Change, 3(3), 283–287, doi:10.1038/nclimate1702, 2012.

Carrasco, L. R., Larrosa, C., Milner-Gulland, E. J., and Edwards, D. P.: A double-edged sword for tropical forests, Science, 346(6205), 38-40, 2014.

Combres, J.-C., Pallas, B., Rouan, L., Mialet-Serra, I., Caliman, J.-P., Braconnier, S., Soulie, J.-C., and Dingkuhn, M.: Simulation of inflorescence dynamics in oil palm and estimation of environment-sensitive phenological phases: a model based analysis, Functional Plant Biology, 40(3), 263-279, 2013.

Corley R. H. V. and Tinker, P. B. (Eds.): The oil palm, 4th edition, Blackwell Science, Oxford, 2003.

Dee, D. P., Uppala, S. M., Simmons, A. J., Berrisford, P., Poli, P., Kobayashi, S., ... and Vitart, F.: The ERA-Interim reanalysis: Configuration and performance of the data assimilation system, Quarterly Journal of the Royal Meteorological Society, 137(656), 553-597, 2011.

Drewniak, B., Song, J., Prell, J., Kotamarthi, V. R., and Jacob, R.: Modeling agriculture in the community land model, Geoscientific Model Development, 6(2), 495-515, doi:10.5194/gmd-6-495-2013, 2013.

Euler, M.: Oil palm expansion among Indonesian smallholders - adoption, welfare implications and agronomic challenges, Ph.D. thesis, University of Göttingen, Germany, 145 pp., 2015.

FAO. FAOSTAT Database, Food and Agriculture Organization of the United Nations, Rome, Italy, available at: http://faostat.fao.org/site/339/default.aspx (last access: 17 June 2015), 2013.

Galloway, J. N., Dentener, F. J., Capone, D. G., Boyer, E. W., Howarth, R. W., Seitzinger, S. P., ... and Vörösmarty, C. J.: Nitrogen cycles: past, present, and future, Biogeochemistry, 70(2), 153-226, 2004.

Georgescu, M., Lobell, D. B., and Field, C. B.: Direct climate effects of perennial bioenergy crops in the United States, Proceedings of the National Academy of Sciences, 108(11), 4307-4312, 2011.

Goh K. J.: Climatic requirements of the oil palm for high yields, in: Managing oil palm for high yields: agronomic principles, Goh K.J. (Eds.), pp. 1–17, Malaysian Soc. Soil Sci. and Param Agric. Surveys, Kuala Lumpur, 2000.

Gunarso, P., Hartoyo, M. E., Agus, F., and Killeen, T. J.: Oil Palm and Land Use Change in Indonesia, Malaysia, and Papua New Guinea. In: Killeen T, Goon J, editors. Reports from the Science Panel of the Second GHG Working Group of the Rountable for Sustainable Palm Oil (RSPO). Kuala Lumpur, 2013.

Hallé, F., Oldeman, R. A. A. and Tomlinson, P. B.: Tropical trees and forests. An architectural analysis. Springer-Verlag, Berlin, 441 pp., 1978.

Hijmans, R. J., Cameron, S. E., Parra, J. L., Jones, P. G., and Jarvis, A.: Very high resolution interpolated climate surfaces for global land areas, International journal of climatology, 25(15), 1965-1978, 2005.

Hoffmann, M. P., Vera, A. C., Van Wijk, M. T., Giller, K. E., Oberthür, T., Donough, C., and Whitbread, A. M.: Simulating potential growth and yield of oil palm (Elaeis guineensis)

with PALMSIM: Model description, evaluation and application, Agricultural Systems, 131, 1-10, 2014.
Hormaza, P., Fuquen, E. M., and Romero, H. M.: Phenology of the oil palm interspecific hybrid Elaeis oleifera × Elaeis guineensis, Scientia Agricola, 69(4), 275-280, 2012.
Huth, N. I., Banabas, M., Nelson, P. N., and Webb, M.: Development of an oil palm cropping systems model: lessons learned and future directions, Environ. Modell. Softw., 62, 411–419, doi:10.1016/j.envsoft.2014.06.021, 2014.
Jin, J. M. and Miller, N. L.: Regional simulations to quantify land use change and irrigation impacts on hydroclimate in the California Central Valley, Theoretical and Applied Climatology, 104, 429-442, 2011.
Koh, L. P. and Ghazoul, J.: Spatially explicit scenario analysis for reconciling agricultural expansion, forest protection, and carbon conservation in Indonesia, P. Natl. Acad. Sci. USA, 107, 11140–11144, doi: 10.1073/pnas.1000530107, 2010.
Kotowska, M. M., Leuschner, C., Antono, T., Meriem, S., and Hertel, D.: Quantifying aboveand belowground biomass carbon loss with forest conversion in tropical lowlands of Sumatra (Indonesia), Global Change Biol., accepted, doi: 10.1111/gcb.12979, 2015a.
Kotowska, M. M., Leuschner, C., Triadiati, T., and Hertel, D.: Conversion of tropical lowland forest lowers nutrient return with litterfall, and alters nutrient use efficiency and seasonality of net primary productivity, Oecologia, submitted, 2015b.
Koven, C. D., Riley, W. J., Subin, Z. M., Tang, J. Y., Torn, M. S., Collins, W. D., Bonan, G. B., Lawrence, D. M., and Swenson, S. C.: The effect of vertically resolved soil biogeochemistry and alternate soil C and N models on C dynamics of CLM4, Biogeosciences, 10(11), 7109-7131, doi:10.5194/bg-10-7109-2013, 2013.
Legros, S., Mialet-Serra, I., Caliman, J. P., Siregar, F. A., Clement-Vidal A., and Dingkuhn, M.: Phenology and growth adjustments of oil palm (Elaeis guineensis) to photoperiod and climate variability, Annals of Botany 104, 1171–1182. doi:10.1093/aob/mcp214, 2009.
Levis, S., Bonan, G., Kluzek, E., Thornton, P., Jones, A., Sacks, W., and Kucharik, C.: Interactive crop management in the Community Earth System Model (CESM1): Seasonal influences on land-atmosphere fluxes, J. Climate, 25, 4839-4859, DOI:10.1175/JCLI-D-11-00446.1., 2012.
Luyssaert, S., Schulze, E. D., Börner, A., Knohl, A., Hessenmöller, D., Law, B. E., Ciais, P., and Grace, J.: Old-growth forests as global carbon sinks, Nature, 455(7210), 213-215, 2008.
Miettinen, J., Shi, C. H. and Liew, S. C.: Deforestation rates in insular Southeast Asia between 2000 and 2010, Global Change Biology, 17, 2261-2270, 2011.
Navarro, M. N. V., Jourdan, C., Sileye, T., Braconnier, S., Mialet-Serra, I., Saint-Andre, L., ... and Roupsard, O.: Fruit development, not GPP, drives seasonal variation in NPP in a tropical palm plantation, Tree physiology, 28(11), 1661-1674, 2008.
Oleson, K. W., Bonan, G. B., Levis, S., and Vertenstein, M.: Effects of land use change on North American climate: impact of surface datasets and model biogeophysics, Climate Dynamics, 23, 117-132, 2004.
Oleson, K., Lawrence, D., Bonan, G., Drewniak, B., Huang, M., Koven, C., Levis, S., Li, F., Riley, W., Subin, Z., Swenson, S., Thornton, P., Bozbiyik, A., Fisher, R., Heald, C., Kluzek, E., Lamarque, J.-F., Lawrence, P., Leung, L., Lipscomb, W., Muszala, S., Ricciuto, D., Sacks,W., Sun, Y., Tang, J., and Yang, Z.-L.: Technical description of version 4.5 of the Community Land Model (CLM), National Center for Atmospheric Research, Boulder, Colorado, USA, 420 pp., doi:10.5065/D6RR1W7M, 2013.
Tang, J. Y., Riley, W. J., Koven, C. D., and Subin, Z. M.: CLM4-BeTR, a generic biogeochemical transport and reaction module for CLM4: model development, evaluation, and application, Geosci. Model Dev., 6, 127-140. doi:10.5194/gmd-6-127-2013, 2013.
van Kraalingen, D. W. G., Breure, C. J., and Spitters, C. J. T.: Simulation of oil palm growth and yield, Agricultural and forest meteorology, 46(3), 227-244, 1989.

766 Veldkamp, E., and Keller, M.: Nitrogen oxide emissions from a banana plantation in the
767 humid tropics, Journal of Geophysical Research: Atmospheres (1984–2012), 102(D13),
768 15889-15898, 1997.
769 von Uexküll, H., Henson, I.E., and Fairhurst, T.: Canopy management to optimize yield, in:
770 Oil Palm: Management for Large and Sustainable Yields, Fairhurst, T., and Härdter, R.
771 (Eds.), Potash & Phosphate Institute of Canada, Potash & Phosphate Institute,
772 International Potash Institute, Singapore, pp. 163-180, 2003.
773 White, M. A., Thornton, P. E., and Running, S. W.: A continental phenology model for
774 monitoring vegetation responses to interannual climatic variability, Global Biogeochem.
775 Cycles, 11, 217-234, 1997.
776

Supplementary materials

Description of the oil palm phenology

The following sections describe the life cycle of each phytomer as well as the planting, stem and root turnover, and rotation (replanting) for the whole plant. Nitrogen retranslocation is implemented for each phytomer during its senescence. Summary of new phenological parameters introduced for the oil palm PFT is in Table A1 in the Appendix.

1. Planting and leaf initiation

Planting is implemented in the similar way as in the CLM4.5 crop phenology except that GDD_{15} is tracked since planting and an option of transplanting is enabled. An initial phytomer emergence threshold (GDD_{init}) is prescribed for attaining the first leaf initiation after planting (Table A1). When GDD_{init} is zero, it implies transplanting from nursery instead of seed sowing in the field. Oil palm seedlings usually grow in nursery for 1-2 year before being transplanted into the field. Therefore, in this study GDD_{init} is set to zero and the first new phytomer is assumed to initiate immediately after transplanting in the field. An initial total LAI of 0.15 is assigned to the existing expanded phytomers, whose leaf sizes are restricted to be within 10% of $PLAI_{max}$ (Table A2).

The oil palm phytomers initiate as leaf primordia in the apical bud and then appear as leaves on the stem successively according to relatively stable intervening periods, termed plastochron (the duration in terms of heat unit (GDD) between successive leaf initiation events) and phyllochron (the rate of leaf emergence from the apical bud). Here for simplicity, the phyllochron is assumed equal to the plastochron. As the apical buds in palms usually do not start to accumulate dry mass immediately after physiological initiation but wait until several phyllochrons before expansion (Navarro et al., 2008), we define leaf initiation as the

start of active accumulation of leaf C in this model, so that the phenological steps and C and N allocation process can be at the same pace.

A parameter *phyllochron* is prescribed with an initial value of 130 degree-days at planting with reference to GDD_{15} and it increases linearly to 1.5 times at 10-year old (Huth et al., 2014; von Uexküll et al., 2003). Given GDD_{init} and *phyllochron*, a heat unit index H_p^{init} for triggering leaf initiation can be calculated for each new phytomer when a preceding phytomer initiates:

$$\begin{aligned} H_1^{init} &= GDD_{init} \\ H_{p+1}^{init} &= H_p^{init} + phyllochron \end{aligned} \qquad \text{Eq. S1}$$

where subscripts *p* and *p+1* refer to successive phytomers and *1* refers to the first new phytomer initiated after planting.

As the GDD accumulates since planting, new phytomers will be turned on in sequence when $GDD_{15} > H_p^{init}$, and will enter the 7-step life cycle one by one. The timing of later phenological steps for each new phytomer is determined at the time of initiation by adding the length of a corresponding phase period (Table A1). Each newly initiated phytomer is assigned a negative rank of $-N$ and remains packed in the bud until the next phase of leaf expansion is triggered. The oldest unexpanded phytomer (spear leaf), right before expansion, has a rank of -1. The GDD period between leaf initiation and expansion is used to calculate the number of bud phytomers that have already initiated before transplanting, i.e. $N = \frac{GDD_{exp}}{phyllochron}$.

2. Leaf expansion

During the phase from initiation to leaf expansion, leaf C already starts to build-up in the bud or spear leaf but it remains photosynthetically inactive. The thermal threshold for leaf expansion is calculated by $H_p^{exp} = H_p^{init} + GDD_{exp}$. Only when $GDD_{15} > H_p^{exp}$ for a

phytomer ranked −1, the leaf starts to expand and becomes photosynthetically active. Its rank changes to a positive value of 1, while the ranks of other phytomers all increase by 1 at the same time. The expansion phase lasts for roughly 5-6 phyllochrons until leaf maturity (Legros et al., 2009).

Hereafter, the pre-expansion and post-expansion growth periods, distinguished by negative and positive ranks, are treated separately so as to differentiate non-photosynthetic and photosynthetic increases in leaf C. The following post-expansion phases and their thresholds are determined with reference to H_p^{exp}.

3. Leaf maturity

Another phenological step is added for the timing of leaf maturing so as to control the period of post-expansion leaf growth for each phytomer. An oil palm leaf usually reaches maturity well before fruit-fill starts on the same phytomer. Therefore, we set the parameter $GDD_{L.mat}$ to be smaller than $GDD_{F.fill}$ (Table A1) so that post-expansion leaf growth continues for 2-3 months (5-6 phyllochrons) and stops around 6 months before fruit-fill. The phenological threshold $H_p^{L.mat}$ is calculated as $H_p^{L.mat} = H_p^{exp} + GDD_{L.mat}$.

4. Fruit filling

Fruit-fill starts on a phytomer when GDD_{15} exceeds a heat unit index $H_p^{F.fill}$. This threshold is calculated by $H_p^{F.fill} = H_p^{exp} + GDD_{F.fill}$. At this point, the phytomer enters reproductive growth. Growth allocation increases gradually for the fruit component while leaf C and LAI remain constant on the mature phytomer until senescence. Due to the fact that most inflorescences on the initial phytomers within 2 years after planting are male (Corley and Tinker, 2003), another threshold GDD_{min} is used to control the beginning of first fruiting on the palm. Only when $GDD_{15} > GDD_{min}$, the mature phytomers are allowed to start fruit-filling.

5. Fruit harvest and output

Fruit harvest occurs at one time step when a phytomer reaches fruit maturity, measured by a heat unit index $H_p^{F.mat} = H_p^{exp} + GDD_{F.mat}$. Since GDD build-up is weather dependent and phyllochron increases through aging, the harvest interval is not constant. New variables track the flow of fruit C and N harvested from each phytomer to PFT-level crop yield output pools. The fruit C and N outputs are isolated and are not involved in any further processes such as respiration and decomposition, although their fate is largely uncertain.

6. Litter fall

For oil palm, leaf litter-fall is performed in two phases: senescence and pruning. Senescence is simulated as a gradual reduction in photosynthetic leaf C and N on the bottom phytomers when $GDD_{15} > H_p^{L.sen}$, where $H_p^{L.sen} = H_p^{exp} + GDD_{L.sen}$. These phytomers are allowed to stay on the palm until pruning is triggered. Their senescence rates are calculated as the inverse of the remaining time until the end of a phytomer's life cycle (GDD_{end}). Leaf C removed during this phase is not put into the litter pool immediately but saved in a temporary pool $C_{leaf}^{senescent}$ until pruning, while the photosynthetic LAI of senescent phytomers are updated at every time step. The reason to do this is that each oil palm frond is a big leaf attached tightly to the stem and its leaflets do not fall to the ground during senescence unless the whole frond is pruned. Thus, the dynamics of soil litter pool and decomposition process could be represented better with this function. Nitrogen from senescent phytomers is remobilized to a separate N retranslocation pool that contributes to photosynthetic N demand of other phytomers and avoids supplying excessive amount of N to the litter. The proportion of N remobilized from senescent leaves before pruning is adjusted by the length of senescent period ($GDD_{end} - GDD_{L.sen}$) with a given pruning frequency, and the rest N goes to the litter pool.

Pruning is conducted at one time step if the number of expanded phytomers (including senescent ones) exceeds the maximum number allowed (i.e. *mxlivenp*). All senescent phytomers are subject to pruning at the time of harvest and their remaining C and N together with the temporary $C_{leaf}^{senescent}$ pool are moved to the litter pool immediately. The frequency and intensity of pruning is determined through the combination of *mxlivenp*, $GDD_{L.sen}$ and *phyllochron*. A larger *mxlivenp* gives lower pruning frequency and a smaller $GDD_{L.sen}$ results in more senescent leaves being pruned at one time. Besides, since *phyllochron* increases by age, the rate of phytomer emergence decreases and thus pruning frequency also decreases when the plantation becomes older.

7. Stem, roots and rotation

Unlike other crops, the oil palm stem is represented by two separate pools for live and dead stem tissues (Fig. 1a). Although the stem of oil palm is not truly woody, field observations have found that the stem section below the lowest phytomer only contains less than 6% of live tissues in the core of trunk for transporting assimilates to the roots (van Kraalingen et al., 1989). This is similar to the stem of most woody trees that largely consists of functionally dead lignified xylem. Therefore, conversion from live to dead stem for oil palm follows the CLM stem turnover function for trees, except that the turnover rate is slightly adjusted to be the inverse of leaf longevity (in seconds), such that when a leaf is dead the stem section below it will mostly become dead. Leaf longevity is around 1.6 years measured from leaf expansion to the end of senescence. The oil palm fine-root turnover follows the CLM scheme for trees and crops which also uses a turnover rate as the inverse of leaf longevity. When the maximum plantation age (usually 25 years) of oil palm is reached and a new rotation cycle starts, the whole PFT is turned off and all C and N of the leaves, stem and roots go to litter. Existing fruit C and N of mature phytomers go to the fruit output pools. The PFT is then replanted in the next year and enters new phenological cycles.